Scientific Journal of Informatics
Vol. 13, No. 3, August 2026
p-ISSN 2407-7658 http://journal.unnes.ac.id/nju/index.php/sji e-ISSN 2460-0040

Boundary-Aware Learning for Glioma Detection in MRI Using YOLOv8 Segmentation Supervision

Muhammad Nurbaitullah[1]*, Abdul Syukur [2], Ahmad Zainul Fanani [3]
[1,2,3]Information Technology Department, Universitas Dian Nuswantoro Semarang, Indonesia

Abstract.
Purpose: Since glioma is the most aggressive and infiltrative type of brain tumor, its detection in magnetic resonance imaging (MRI) is especially difficult. Despite the excellent overall accuracy for brain tumor detection with YOLOv8-based object detection, the glioma-specific performance is limited owing to ambiguity of tumor boundaries. This work seeks to elucidate if boundary-aware learning can enhance glioma detection beyond typical bounding box–based approaches.
Methods: This study focuses exclusively on glioma detection using the Cheng brain tumor MRI dataset. YOLOv8 is used as the baseline detector, and boundary-aware learning is implemented through segmentation supervision using YOLOv8-Seg by leveraging pixel-level tumor masks. All the experiments are done in a standardized training environment to allow fair and unbiased comparison.
Result: Experimental evaluation shows that YOLOv8-Seg achieved a detection precision of 0.899, recall of 0.905, and mAP@50 of 0.940, while segmentation results achieved a mask precision of 0.900, recall of 0.904, and mAP@50 of 0.943. For glioma-specific analysis, the model achieved a box mAP@50 of 0.875 and a mask mAP@50 of 0.877. These results indicate that segmentation supervision improves spatial boundary representation even though improvements in conventional detection metrics remain marginal.
Novelty: Unlike the other works that are based on augmentation of the data and performance of better detection, this work has devised a glioma-centric design, and shows bounding box-based detection is insufficient. This work highlights the need for considering boundary aware learning applying the supervision of segmentation in the automated glioma detection system, which can improve the reliability and interpretability of the system.

Keywords: Glioma Detection; Magnetic Resonance Imaging; YOLOv8; Segmentation Supervision; Boundary-Aware Learning
Received March 2026 / **Revised** April 2026 / **Accepted** April 2026

INTRODUCTION

Glioma is the most aggressive and infiltrative tumor of the central nervous system. Glioma has the characteristic of heterogeneous internal structures and diffuse tumor margins that render accurate delineation challenging in magnetic resonance imaging (MRI) [1], [2]. The infiltrative growth pattern of glioma frequently causes low contrast between tumor and healthy tissue, and it poses great difficulty for manually applied analysis as well as automation of these analyses [3]. Accurate localization of tumor and tumor localization issues, important for diagnosis, therapeutics and disease detection, are so vital in diagnosing and treating and monitored glioma that computer-aided detection systems for glioma remain a matter of continued study [4].

Recent breakthroughs in deep learning have significantly advanced automated analysis of brain tumors, in particular by advanced convolutional neural network and transformer-based architectures [5], [6] and significantly helped in the automation of automated brain tumor processing. Within these lines of research, object detection models are gradually gaining attention for it capability of locating tumor areas in a efficient manner without the need for dense pixel-level annotations [7]. The YOLO-based detectors, such as YOLOv8 architecture, are commonly used in medical imaging because they provide good compromise between detection accuracy and computational efficiency [8]. YOLO-based models have been well performed as multi-class brain tumor detection in MRI for both large-scale and near real-time clinically, reported in several recent studies, [9], [10].

Despite these advances, most existing YOLO-based brain tumor detection studies emphasize aggregate performance across different tumor types, such as meningioma, glioma, and pituitary tumors [10], [11]. In

[1]*Corresponding author.
Email addresses: p31202402601@mhs.dinus.ac.id (Nurbaitullah), abah.syukur01@dsn.dinus.ac.id (Syukur), a.zainul.fanani@dsn.dinus.ac.id (Fanani)
DOI: 10.15294/sji.v13i3.42307

such multi-class settings, improvements in detection metrics are often dominated by tumors with compact shapes and well-defined boundaries, while the specific challenges associated with glioma are not explicitly addressed [12]. As a result, glioma-related detection limitations may be obscured by high overall accuracy, leading to an overestimation of model reliability for infiltrative tumors [13].

Several recent studies have applied YOLO-based detectors for brain tumor analysis. For instance, Passa et al. [10] utilized YOLOv8 combined with data augmentation techniques for multi-class brain tumor detection and reported a mAP@50 exceeding 0.92 on the Cheng MRI dataset. Similarly, Hossain R et al. [8] implemented deep learning–based object detection for tumor localization and achieved high classification accuracy across meningioma, glioma, and pituitary tumors. However, these studies mainly focused on improving overall detection accuracy and did not explicitly analyze the challenges associated with infiltrative tumor boundaries, particularly in glioma cases. Consequently, improvements in aggregate metrics may mask the model's limitations in accurately representing diffuse tumor margins.

In contrast, segmentation-based approaches such as nnU-Net [14] have demonstrated superior capability in capturing detailed tumor boundaries through pixel-level supervision. These methods emphasize boundary-sensitive learning mechanisms, enabling more accurate delineation of irregular tumor shapes. However, segmentation models typically require dense annotations and higher computational cost, limiting their integration into real-time detection frameworks. Therefore, integrating segmentation supervision into object detection architectures such as YOLOv8 may offer a balanced solution between localization efficiency and boundary awareness.

From a clinical and radiological perspective, glioma differs fundamentally from other brain tumors due to its diffuse margins and complex spatial extent [15]. Bounding box–based supervision, which represents tumors using coarse rectangular regions, is inherently limited in capturing these characteristics [16]. A rectangular bounding box cannot accurately describe the true tumor extent and often includes surrounding healthy tissue, introducing ambiguity during training [14]. Consequently, object detection models trained solely with bounding box annotations may fail to learn meaningful boundary representations for glioma, resulting in localization errors and reduced interpretability [17].

In contrast, segmentation-based approaches provide pixel-level delineation of tumor boundaries and have become the dominant paradigm for glioma analysis, as demonstrated by recent benchmarks and segmentation frameworks [18], [19]. State-of-the-art segmentation models emphasize boundary-sensitive learning to better characterize infiltrative tumor morphology [20]. These findings suggest that boundary information plays a critical role in accurate glioma representation and may be necessary to overcome the limitations of detection-only supervision [21].

However, the integration of segmentation supervision into contemporary object detection frameworks for glioma remains relatively underexplored. Most recent YOLOv8-based studies prioritize data augmentation strategies, architectural refinements, or loss function optimization to improve detection performance, while boundary-aware learning mechanisms are rarely investigated [11], [22]. As a result, it remains unclear whether incorporating segmentation supervision into a detection framework can provide more informative spatial representations for glioma without altering the dataset or experimental conditions [23].

Therefore, this study addresses this gap by conducting a glioma-centric investigation into boundary-aware learning using segmentation supervision within a YOLOv8-based detection framework. Unlike previous works that primarily focus on maximizing overall detection accuracy, this research examines whether segmentation supervision can enhance spatial representation and interpretability of glioma detection beyond conventional bounding box–based approaches. The objective of this study is to evaluate the effectiveness of segmentation-supervised YOLOv8 in modeling infiltrative tumor boundaries under controlled and fair experimental settings.

METHODS

Research design

This study uses experimental research design to study boundary-aware learning for the detection of glioma in magnetic resonance imaging (MRI). The experimental pipeline in Figure 1 presents the overall workflow from dataset preparation to model training and evaluation. The primary objective of this study is not to maximize overall detection accuracy, but to examine the representational limitations of bounding

box–based supervision for infiltrative glioma tumors and to evaluate the contribution of segmentation supervision to spatial representation quality.

To ensure methodological rigor and unbiased comparison, an apple-to-apple evaluation strategy is adopted, where all experimental settings are kept identical across models except for the supervision mechanism. This strategy minimizes confounding variables and is commonly recommended in medical image analysis studies for fair methodological comparison [24].

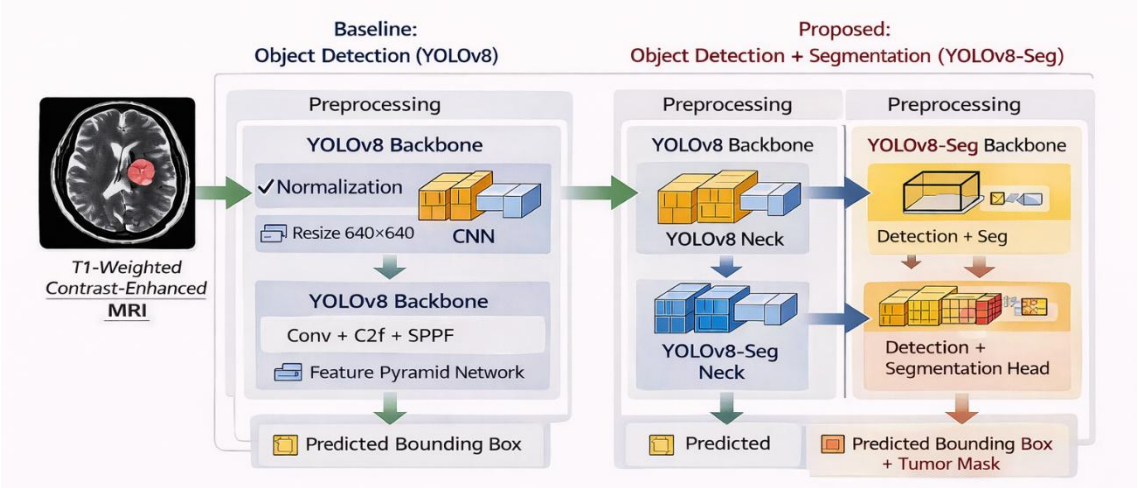

Figure 1. Overview of the proposed

Dataset description

The experiments are conducted using the Cheng brain tumor MRI dataset, which consists of T1-weighted contrast-enhanced MRI images with expert-annotated pixel-level tumor masks [25]. The dataset comprises three tumor categories: meningioma, glioma, and pituitary tumors. This study consists of a glioma-centric evaluation based on non-glioma tumor classes maintained for the realistic clinical scenario and evaluation of class discrimination ability [26].

Table 1. Summary of the dataset

Item	Description
Imaging modality	T1-weighted contrast-enhanced MRI
Tumor category	Meningioma, Glioma, Pituitary
Dataset source	Cheng brain tumor dataset
Total images	691
Annotation type	Pixel-level tumor mask
Bounding box	Derived from tumor mask
Evaluation scope	Glioma-centric analysis

Table 1 summarizes the features of the dataset encompassing imaging modality, tumor categories, annotation type, and evaluation scope. The number of images and class distribution employed in this study is presented in Table 2, where glioma and non-glioma samples are clearly distinguished.

For each MRI image, a binary tumor mask is provided. Bounding box annotations are automatically generated by computing the minimum enclosing rectangle around each tumor mask. This procedure reduces annotation subjectivity and labeling noise, which are common challenges in medical object detection tasks [27]. The dataset is divided into training, validation, and testing subsets with a fixed split ratio of 70%, 20%, and 10%, respectively. The same split is consistently used for all experiments.

Table 2. Dataset distribution

Class	Number of Sample
Glioma	324
Non-Glioma	357

Baseline model: YOLOv8 detection
The baseline detection model used in this study is YOLOv8, a single-stage object detection framework composed of a backbone network, a neck for multi-scale feature fusion, and a detection head for bounding box regression and class prediction. Figure 1 shows the structural aspects of the baseline model.

In this system, the backbone utilizes convolutional layers and C2f modules to extract hierarchical feature representations from input MRI images. In order to increase multi-scale contextual information, a Spatial Pyramid Pooling Fast (SPPF) module is implemented at the end of the backbone, to enable the model to capture tumors of varying sizes [28].

Feature aggregation is performed using a Feature Pyramid Network (FPN) combined with a Path Aggregation Network (PAN), allowing effective fusion of feature maps at different spatial resolutions [29]. This design is particularly important for glioma detection due to significant variability in tumor size and shape [30].

In the baseline configuration, the detection head is trained exclusively using bounding box annotations derived from tumor masks. No pixel-level boundary information is provided during training. As a result, the model learns coarse rectangular tumor representations, which are insufficient for accurately modeling infiltrative glioma margins.

Proposed detection framework
For the boundary-aware learning, this work uses YOLOv8-Seg that implements a segmentation branch supervised with pixel-level tumor masks [28]. Besides predicting both bounding boxes and class probabilities, YOLOv8-Seg produces segmentation masks that explicitly encode tumor boundary information during training.

All training configurations are kept uniform and identical among the methods, such as input image resolution, optimizer, learning rate, batch size, and number of epochs. The detailed training configuration adopted for all experiments is summarized in Table 3. This ensures that performance differences are only due to supervision strategy and not to variability in the course of training [31]. Different methods of data augmentation (flipping, scaling, intensity variation) are applied uniformly across models to ensure that differences in performance relate to supervision approach.

Table 3. Training configuration

Parameter	Value
Framework	Ultralytics YOLOv8
Model variants	YOLOv8 (Detection), YOLOv8-Seg
Input image size	640 × 640
Optimizer	AdamW
Learning rate	Default YOLOv8 setting
Batch size	As supported by GPU memory
Number of epochs	Fixed across all experiments
Data augmentation	Flip, scale, intensity variation
Hardware	Google Colab (GPU)

Performance evaluation metrics
To quantify the achieved performance, the proposed model was evaluated using the metrics regularly used detection research, i.e., YOLO-based deep learning systems [3], [6], [11]. The chosen metrics are Intersection-over-Union (IoU), Precisionffc, Recall, and mean Average Precision (mAP) at IoU thresholds of 0.50 and 0.50–0.95. These measures allow the detection accuracy, localization consistency, and classification performance of all model configurations to be objectively measured.

1) Precision
   Precision indicates the ratio of the number of correctly predicted defect examples out of all detected predictions. It is defined as:

$$Precision = \frac{TP}{TP + FP} \tag{4}$$

   where:

- TP= True Positives
- FP= False Positives

More precision means lower false alarms, and low precision can lead to inappropriate product rejection in automated inspection systems [22].

2) Recall

Recall checks the model's capability to detect all instances of true objects in existence and is defined as:

$$Recall = \frac{TP}{TP + FN} \tag{5}$$

where:

- FN= False Negatives

Recall is crucial in situations where the detection of defects might cause failure, as identified in industrial safety-critical environments that may require high recall [23], [24].

3) Average Precision (AP)

Average Precision (AP) is computed from the area under the Precision-Recall curve. The continuous integral form is expressed as:

$$AP = \int_0^1 P(R)\, dR \tag{6}$$

where $P(R)$represents precision as a function of recall.
In practice, AP is computed using discrete recall thresholds:

$$AP = \sum_{n=1}^{N} (R_n - R_{n-1}) \cdot P_n \tag{7}$$

4) Mean Average Precision (mAP)

The final metric, mean Average Precision, provides the overall detection score across all classes [29]. It is computed as:

$$mAP = \frac{1}{C} \sum_{i=1}^{C} AP_i \tag{8}$$

where:

- C= number of object classes
- AP_i= Average Precision for class i

RESULT AND DISCUSSION

Quantitative performance evaluation

The performance of the proposed segmentation-supervised detection framework was measured quantitatively by conventional object detection and segmentation metrics such as Precision, Recall, mAP@50, and mAP@50–95, defined in Equations (4 - 8). Table 4 summarizes the results of this evaluation on YOLOv8-Seg from bounding box detection to segmentation mask prediction.

Table 4. Comparison with previous studies

Study	Model	Dataset	mAP@50	Approach
Passa et al. [10]	YOLOv8	Cheng MRI	0.894	Data augmentation
Talo et al. [8]	CNN Detector	Cheng MRI	0.90	Object detection
This study	**YOLOv8-Seg**	**Cheng MRI**	**0.943**	**Segmentation supervision**

Compared with previous YOLO-based studies, the proposed segmentation-supervised detection framework achieves competitive detection performance while additionally providing boundary-aware spatial representation. Unlike prior works that mainly rely on data augmentation or architectural modifications, this study focuses on improving boundary representation through segmentation supervision.

Table 5. Performance comparison (YOLOv8-Seg)

Model	Task	Precision	Recall	mAP@50	mAP@50–95
YOLOv8-Seg	Detection (Box)	0.899	0.905	0.940	0.685
YOLOv8-Seg	Segmentation (Mask)	0.900	0.904	0.943	0.672

Using metrics reported in Table 4, the overall performance of YOLOv8-Seg can be seen in tumor localization with box-based Precision 0.899, Recall 0.905, and mAP@50 of 0.940. The model has a mask-based Precision of 0.900, Recall of 0.904, and mAP@50 of 0.943 in segmentation, demonstrating that pixel-level supervision leads to precise delineation of tumor regions. However, a decrease in mAP@50–95 is observed for segmentation results compared to bounding box detection, reflecting increased difficulty in achieving high-overlap localization for infiltrative tumor boundaries.

To provide a more focused evaluation, class-wise performance analysis is conducted with particular emphasis on glioma cases. The quantitative results for glioma detection and segmentation are presented in Table 5. As shown in the table 6, the glioma class achieves a box mAP@50 of 0.875 and a mask mAP@50 of 0.877. While segmentation supervision provides a marginal improvement at lower IoU thresholds, a noticeable reduction in mAP@50–95 is observed for mask prediction. This trend suggests that precise boundary delineation for glioma remains challenging at stricter IoU thresholds, consistent with the diffuse and infiltrative nature of glioma tumors.

Table 6. Glioma detection performance (YOLOv8-Seg)

Class	Task	Precision	Recall	mAP@50	mAP@50–95
Glioma	Box	0.852	0.830	0.875	0.594
Glioma	Mask	0.852	0.826	0.877	0.558

In summary, the quantitative results show that segmentation supervision does not translate to significant numerical gains in aggregate detection metrics. Instead, the performance trends indicate that the baseline YOLOv8 detector has reached a saturation point, where additional supervision yields limited improvements in conventional evaluation scores.

Confusion matrix analysis

Confusion matrix analysis of the segmentation-supervised model is performed to investigate class-specific behavior and misclassification patterns. The resulting confusion matrix is illustrated in Figure 2.

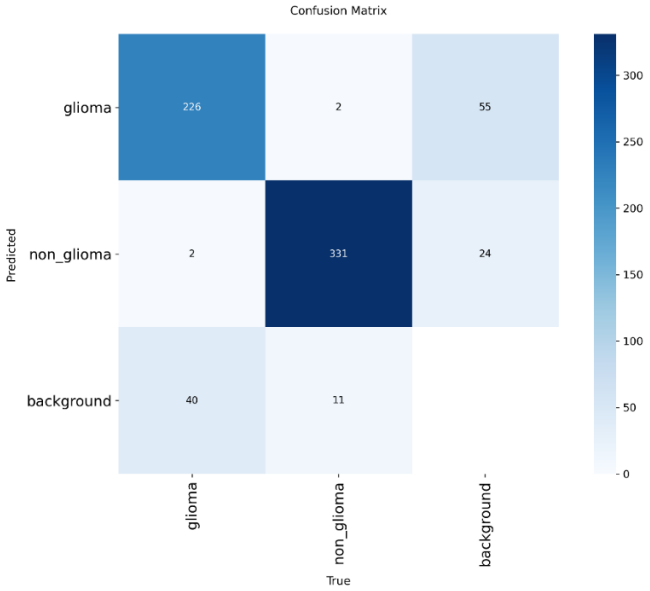

Figure 2. Confusion matrix

As shown in Figure 2, the majority of misclassifications involving glioma occur between glioma and background classes, rather than between glioma and other tumor types such as meningioma or pituitary tumors. This observation indicates that inter-class similarity is not the primary source of error. Instead, the dominant challenge arises from ambiguous tumor boundaries and diffuse margins, which cause glioma regions to be partially detected or misclassified as background.

These results highlight that bounding box–based localization struggles to capture the true spatial extent of glioma tumors, reinforcing the motivation for incorporating segmentation supervision to address boundary ambiguity.

Qualitative analysis

To complement the quantitative evaluation, qualitative visualization is conducted to compare localization characteristics between the baseline YOLOv8 detector and the segmentation-supervised YOLOv8-Seg model. Representative examples are presented in Figure 3, including the original MRI images, detection results from the YOLOv8 baseline, and segmentation outputs from YOLOv8-Seg.

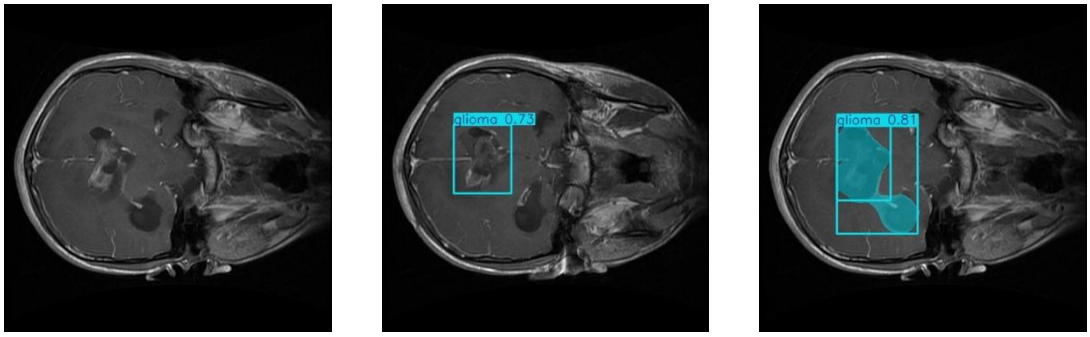

(a) Original MRI (b) YOLOv8 baseline (c) YOLOv8-Seg

Figure 3. Qualitative comparison of YOLOv8 and YOLOv8-Seg

As shown in Figure 3, the baseline YOLOv8 model generates coarse bounding boxes, which often cover the surrounding healthy tissue and render the location of the tumor boundaries less precise. In contrast, YOLOv8-Seg generates segmentation masks that more closely follow the actual tumor shape and spatial extent. This qualitative improvement demonstrates that segmentation supervision enhances boundary representation and provides more interpretable localization results, even when numerical detection metrics remain comparable.

The qualitative findings support quantitative observations, indicating that the primary contribution of segmentation supervision lies in improved spatial interpretability rather than significant gains in aggregate detection accuracy.

Discussion

The objective of this study was to investigate whether boundary-aware learning through segmentation supervision can improve the spatial representation of glioma detection in MRI using a YOLOv8-based detection framework. The experimental results indicate that although segmentation supervision does not lead to substantial improvements in conventional detection metrics such as Precision, Recall, and mAP, it provides meaningful advantages in representing the spatial characteristics of infiltrative tumors.

The quantitative results show that YOLOv8-Seg achieved strong detection performance with a box-based mAP@50 of 0.940 and a mask-based mAP@50 of 0.943. However, when focusing specifically on glioma cases, the improvement becomes marginal, where the box-based mAP@50 reaches 0.875 and the mask-based mAP@50 reaches 0.877. These findings suggest that the baseline YOLOv8 detector has already achieved relatively high detection performance, and additional supervision primarily influences how the tumor boundaries are represented rather than significantly improving aggregate detection metrics.

The confusion matrix analysis further reveals that most detection errors occur between glioma and background regions rather than between tumor classes. This pattern indicates that the primary difficulty lies

in the diffuse and infiltrative nature of glioma boundaries rather than inter-class similarity. Similar observations have been reported by Kervadec H et al. [13], who demonstrated that bounding box–based supervision often fails to accurately represent irregular anatomical structures in medical imaging tasks. As a result, object detection models may produce partial localization when applied to tumors with ambiguous margins.

Qualitative visualization results support these observations. While the baseline YOLOv8 detector produces coarse rectangular bounding boxes that frequently include surrounding healthy tissue, the segmentation-supervised YOLOv8-Seg model generates tumor masks that more closely follow the true spatial extent of the tumor. Although these improvements are not fully reflected in conventional detection metrics, they significantly enhance the interpretability and spatial reliability of tumor localization, which is particularly important for clinical decision support systems [19].

Overall, the findings indicate that segmentation supervision improves boundary representation for infiltrative tumors such as glioma, even when numerical detection performance remains relatively stable. This suggests that evaluation of glioma detection models should not rely solely on aggregate detection metrics but should also consider spatial interpretability and boundary representation when assessing model effectiveness.

CONCLUSION

This study investigated the role of boundary-aware learning through segmentation supervision for glioma detection in MRI using a YOLOv8-based framework. Experimental results show that YOLOv8-Seg achieved a detection mAP@50 of 0.940 and a mask mAP@50 of 0.943, while glioma-specific analysis produced a box mAP@50 of 0.875 and a mask mAP@50 of 0.877. These findings indicate that segmentation supervision provides improved spatial representation of tumor boundaries, even though improvements in conventional detection metrics remain limited. The results highlight that bounding box–based detection alone is insufficient for accurately representing the infiltrative nature of glioma tumors. Segmentation supervision improves boundary awareness and interpretability, which are essential for clinically meaningful tumor localization. Future research may explore boundary-aware loss functions and multimodal MRI integration to further enhance tumor boundary delineation in automated glioma detection systems.

REFERENCES

[1] D. N. Louis *et al.*, "The 2021 WHO Classification of Tumors of the Central Nervous System: a summary," *Neuro. Oncol.*, vol. 23, no. 8, pp. 1231–1251, Aug. 2021, doi: 10.1093/neuonc/noab106.

[2] Z. Wang, L. Wang, and Y. Wang, "Radiomics in glioma: emerging trends and challenges," *Ann. Clin. Transl. Neurol.*, vol. 12, no. 3, pp. 460–477, Mar. 2025, doi: https://doi.org/10.1002/acn3.52306.

[3] S. Bauer, R. Wiest, L.-P. Nolte, and M. Reyes, "A survey of MRI-based medical image analysis for brain tumor studies," *Phys. Med. Biol.*, vol. 58, no. 13, p. R97, 2013, doi: 10.1088/0031-9155/58/13/R97.

[4] N. M. Dipu, S. A. Shohan, and K. M. A. Salam, "Deep Learning Based Brain Tumor Detection and Classification," in *2021 International Conference on Intelligent Technologies (CONIT)*, 2021, pp. 1–6. doi: 10.1109/CONIT51480.2021.9498384.

[5] K. Xia and J. Wang, "Recent advances of Transformers in medical image analysis: A comprehensive review," *MedComm – Future Medicine*, vol. 2, no. 1, p. e38, Mar. 2023, doi: https://doi.org/10.1002/mef2.38.

[6] M. Saraei, M. Lalinia, and E.-J. Lee, "Deep Learning-Based Medical Object Detection: A Survey," *IEEE Access*, vol. 13, pp. 53019–53038, 2025, doi: 10.1109/ACCESS.2025.3553087.

[7] J. Zhong, H. Qian, H. Wang, W. Wang, and Y. Zhou, "Improved real-time object detection method based on YOLOv8: a refined approach," *J. Real. Time. Image Process.*, vol. 22, no. 1, p. 4, 2024, doi: 10.1007/s11554-024-01585-8.

[8] R. Hossain, R. B. Ibrahim, and H. B. Hashim, "Automated Brain Tumor Detection Using Machine Learning: A Bibliometric Review," *World Neurosurg.*, vol. 175, pp. 57–68, 2023, doi: https://doi.org/10.1016/j.wneu.2023.03.115.

[9] A. B. Abdusalomov, M. Mukhiddinov, and T. K. Whangbo, "Brain Tumor Detection Based on Deep Learning Approaches and Magnetic Resonance Imaging," *Cancers (Basel).*, vol. 15, no. 16, 2023, doi: 10.3390/cancers15164172.

[10] R. Satila Passa, S. Nurmaini, and D. P. Rini, "YOLOv8 Based on Data Augmentation for MRI Brain Tumor Detection," *Scientific Journal of Informatics*, vol. 10, no. 3, p. 363, 2023, doi: 10.15294/sji.v10i3.45361.

[11] M. I. Jaber *et al.*, "A deep learning image-based intrinsic molecular subtype classifier of breast tumors reveals tumor heterogeneity that may affect survival," *Breast Cancer Research*, vol. 22, no. 1, p. 12, 2020, doi: 10.1186/s13058-020-1248-3.

[12] A. V Bonm, R. Ritterbusch, P. Throckmorton, and J. J. Graber, "Clinical Imaging for Diagnostic Challenges in the Management of Gliomas: A Review," *Journal of Neuroimaging*, vol. 30, no. 2, pp. 139–145, Mar. 2020, doi: https://doi.org/10.1111/jon.12687.

[13] H. Kervadec, J. Dolz, S. Wang, E. Granger, and I. Ben Ayed, "Bounding boxes for weakly supervised segmentation: Global constraints get close to full supervision," in *Proceedings of the Third Conference on Medical Imaging with Deep Learning*, T. Arbel, I. Ben Ayed, M. de Bruijne, M. Descoteaux, H. Lombaert, and C. Pal, Eds., in Proceedings of Machine Learning Research, vol. 121. PMLR, Apr. 2020, pp. 365–381. [Online]. Available: https://proceedings.mlr.press/v121/kervadec20a.html

[14] F. Isensee, P. F. Jaeger, S. A. A. Kohl, J. Petersen, and K. H. Maier-Hein, "nnU-Net: a self-configuring method for deep learning-based biomedical image segmentation," *Nat. Methods*, vol. 18, no. 2, pp. 203–211, 2021, doi: 10.1038/s41592-020-01008-z.

[15] T. Brosch, J. Peters, A. Groth, T. Stehle, and J. Weese, "Deep Learning-Based Boundary Detection for Model-Based Segmentation with Application to MR Prostate Segmentation," in *Medical Image Computing and Computer Assisted Intervention – MICCAI 2018*, A. F. Frangi, J. A. Schnabel, C. Davatzikos, C. Alberola-López, and G. Fichtinger, Eds., Cham: Springer International Publishing, 2018, pp. 515–522.

[16] M. C. de Verdier *et al.*, "The 2024 Brain Tumor Segmentation (BraTS) Challenge: Glioma Segmentation on Post-treatment MRI," May 2024, [Online]. Available: http://arxiv.org/abs/2405.18368

[17] S. Saurav, A. Sharma, R. Saini, and S. Singh, "An attention-guided convolutional neural network for automated classification of brain tumor from MRI," *Neural Comput. Appl.*, vol. 35, no. 3, pp. 2541–2560, 2023, doi: 10.1007/s00521-022-07742-z.

[18] M. Shafique, N. Rahim, J. Ahmad, M. Siadat, K. Malik, and G. Malik, "FocusSDF: Boundary-Aware Learning for Medical Image Segmentation via Signed Distance Supervision," Nov. 2025, [Online]. Available: http://arxiv.org/abs/2511.11864

[19] K. Lakshmi, S. Amaran, G. Subbulakshmi, S. Padmini, G. P. Joshi, and W. Cho, "Explainable artificial intelligence with UNet based segmentation and Bayesian machine learning for classification of brain tumors using MRI images," *Sci. Rep.*, vol. 15, no. 1, p. 690, 2025, doi: 10.1038/s41598-024-84692-7.

[20] Y. Wang, B. Xiao, X. Bi, W. Li, and X. Gao, "Boundary-Aware Prototype in Semi-Supervised Medical Image Segmentation," *IEEE Transactions on Image Processing*, vol. 33, pp. 5456–5467, 2024, doi: 10.1109/TIP.2024.3463412.

[21] L. Yu, W. Min, and S. Wang, "Boundary-Aware Gradient Operator Network for Medical Image Segmentation," *IEEE J. Biomed. Health Inform.*, vol. 28, no. 8, pp. 4711–4723, 2024, doi: 10.1109/JBHI.2024.3404273.

[22] K. Alleman, E. Knecht, J. Huang, L. Zhang, S. Lam, and M. DeCuypere, "Multimodal Deep Learning-Based Prognostication in Glioma Patients: A Systematic Review," *Cancers (Basel).*, vol. 15, no. 2, 2023, doi: 10.3390/cancers15020545.

[23] Md. Ariful Islam, M. F. Mridha, M. Safran, S. Alfarhood, and Md. Mohsin Kabir, "Revolutionizing Brain Tumor Detection Using Explainable AI in MRI Images," *NMR Biomed.*, vol. 38, no. 3, p. e70001, Mar. 2025, doi: https://doi.org/10.1002/nbm.70001.

[24] L. Maier-Hein *et al.*, "Why rankings of biomedical image analysis competitions should be interpreted with care," *Nat. Commun.*, vol. 9, no. 1, p. 5217, 2018, doi: 10.1038/s41467-018-07619-7.

[25] J. Cheng *et al.*, "Correction: Enhanced Performance of Brain Tumor Classification via Tumor Region Augmentation and Partition," *PLoS One*, vol. 10, no. 12, pp. e0144479-, Dec. 2015, [Online]. Available: https://doi.org/10.1371/journal.pone.0144479

[26] M. Li *et al.*, "Artificial intelligence-assisted theranostics for brain tumors: Advancements and future perspectives," *VIEW*, vol. 6, no. 6, p. 20250119, Dec. 2025, doi: https://doi.org/10.1002/VIW.20250119.

[27] L. Ju *et al.*, "Improving Medical Images Classification With Label Noise Using Dual-Uncertainty Estimation," *IEEE Trans. Med. Imaging*, vol. 41, no. 6, pp. 1533–1546, 2022, doi: 10.1109/TMI.2022.3141425.

[28] M. Talib, A. H. Y. Al-Noori, and J. Suad, "YOLOv8-CAB: Improved YOLOv8 for Real-time Object Detection," *Karbala International Journal of Modern Science*, vol. 10, no. 1, pp. 56–68, 2024, doi: 10.33640/2405-609X.3339.

[29] S. Seferbekov, V. Iglovikov, and A. Buslaev, "Feature Pyramid Network for Multi-Class Land Segmentation."

[30] K. He, X. Zhang, S. Ren, and J. Sun, "Spatial Pyramid Pooling in Deep Convolutional Networks for Visual Recognition," *IEEE Trans. Pattern Anal. Mach. Intell.*, vol. 37, no. 9, pp. 1904–1916, 2015, doi: 10.1109/TPAMI.2015.2389824.

[31] Z. Cai, K. Zhou, and Z. Liao, "A Systematic Review of YOLO-Based Object Detection in Medical Imaging: Advances, Challenges, and Future Directions," 2025, *Tech Science Press*. doi: 10.32604/cmc.2025.067994.